

# Fast Optimization Methods in the Selective Cooling of Steel

K. Eppler and F. Tröltzsch

<sup>1</sup> Technische Universität Chemnitz, Fakultät für Mathematik, 09107 Chemnitz

<sup>2</sup> Technische Universität Berlin, Fachbereich Mathematik, Straße des 17. Juni, 10623 Berlin

**Abstract.** We consider the problem of cooling milled steel profiles at a maximum rate subject to given bounds on the difference of temperatures in prescribed points of the steel profile. This leads to a nonlinear parabolic control problem with state constraints in a 2D domain. The controls can admit values from continuous or discrete sets. A method of instantaneous control is applied to establish a fast solution technique. Moreover, continuous and discrete control strategies are compared, and conclusions are given from an applicational point of view.

**Keywords:** Cooling steel, nonlinear heat equation, optimal control, pointwise state constraints, instantaneous control, linear integer programming

**AMS subject classification:** 49M35, 90C10, 65K05, 93C20, 93C95

## 1 Introduction

The selective cooling of steel profiles is an important part of the production process in steel mills. Intelligent future strategies aim to combine a reduction of temperature in the rolled profile with an equalization of its interior temperature distribution. An accelerated optimal cooling will reduce the amount of investment in cooling sections. Moreover, it is able to stabilize the interior structure of the steel during phase transitions. Reducing the temperature in the profile as uniformly as possible leads to a higher quality of the steel.

We believe that the intuition of engineers alone is not able to control this process. The mathematical tools of optimal control theory will be helpful to find optimal cooling strategies.

We have reported on this issue in a number of mathematical papers, for instance in Krengel et.al. [7] or Lezius and Tröltzsch [11], where a method of feasible directions was developed to solve the optimal control problem. The numerical tests confirmed the stability and reliability of the method. However, the computing time was high. Therefore, Tröltzsch and Unger [14] dealt with a very fast and precise suboptimal solution method, where, after discretization, the optimization is reduced to a sequence of low-dimensional linear programming problems. A similar problem was discussed by Landl and Engl [9]. In contrast to the setting in [14], where the intensity of the cooling spray nozzles can be chosen *continuously*, in [9] the cooling is controlled by switching on and off the nozzles. This *discrete* strategy seems to be more adequate for the technical process.

In this paper we investigate the application of continuous as well as of discrete control strategies to the model discussed in [14]. It is not realistic to solve the associated large scale mixed integer programming problem up to the optimal solution in the discrete case. This refers also to the continuous problem. Therefore, we decided to extend the suboptimal method of instantaneous control type from the case of continuously controllable nozzles to discrete 0-1-controls. We will show that the extension can be done in a quite simple and straightforward way:

The core of the suboptimal method of [14] consists of small scale linear programming problems, which have been solved by the simplex method. Here, we arrive at small scale linear *integer* programming problems, which are solved by appropriate methods. Combining this main idea with some special techniques to make the method work, we finally achieved computing times of the same order as for the continuous control strategies. This is important to allow interactive work of the engineer and - at least in principle - an online-control of the cooling process.

Obviously, the restriction to discrete strategies shrinks the set of feasible controls. It is quite natural that integer controls are less flexible than continuous ones. Therefore, in our numerical tests, we increased the number of spray nozzles to compensate for this. However, the numerical experience shows that increasing the number of nozzles alone is not the best solution. Using nozzles of smaller size turned out to be more helpful.

The selective cooling of steel profiles is only one of various applications of control theory in metallurgy. Other important issues are the continuous casting of steel, Engl, Langthaler and Mansellio[2], Grever [4], Laitinen and Neittaanmäki [8], Neittaanmäki [12], the firing of kilns, Leibfritz and Sachs[10], or the Laser hardening of steel, Hömberg and Sokołowski [6].

## 2 The optimal control problem and iterative solution

A cooling line consists of a certain number of cooling segments, where water is sprayed on the surface of the hot steel profile. Each cooling segment is followed by a zone of air cooling equalizing the developed temperature differences. The basic scheme is shown in Figure 1.

In the cooling segments, a certain fixed number of spray nozzles is located in groups around the profile. There can be a sequence of groups in each cooling segment. To explain the mathematical model, let us regard one fixed cross section  $\Omega \subset \mathbb{R}^2$  of the steel profile. We follow its run through the whole cooling line. This causes an internal time scheme for the reference domain  $\Omega$ . The cross section  $\Omega$  enters the first nozzle group of the first cooling segment at time  $t_0 = 0$ . Now the surface is sprayed on by the  $p$  nozzles of the first nozzle group. After leaving this group,  $\Omega$  reaches the second one at time  $t_1$ . (Note that there is a small difference to the notation in [7], therein  $t_1$  denotes the time for passing the first cooling segment.) After  $r$  steps,  $\Omega$  has passed the first cooling segment. Now an area of

air cooling follows. At time  $t_s$  the next cooling segment is entered. Finally, the cross section reaches the end of the last air cooling area at time  $t_K = T$ , where the profile has passed  $M$  zones of water or air cooling.

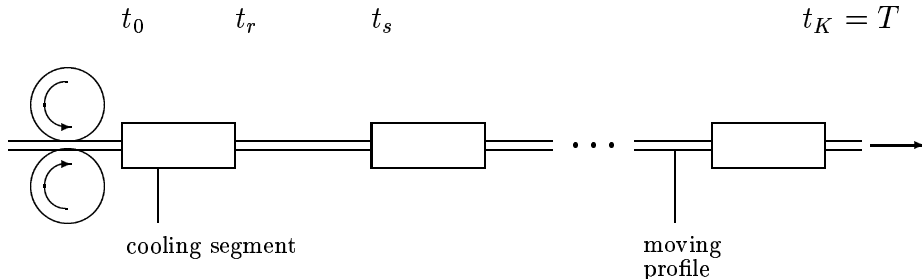


Figure 1: Scheme of a cooling section

To shorten the presentation, we rely on the following simplifications: All cooling segments contain the same number  $r$  of nozzle groups with the same number  $p$  of nozzles. The time for passing any single nozzle group is equal along the whole cooling line. Moreover, the lengths of all cooling segments and air cooling areas are assumed to be equal. Therefore, the time to pass an arbitrary segment is constant. These restrictions are not necessary for the computational technique to work. We adopt them only here to simplify the notation. The resulting discretization of the internal time is given by

$$0 = t_0 < t_1 < \dots < t_r = rt_1 < \dots < t_s = 2t_r < \dots < t_K = Mt_r = T. \quad (1)$$

The heat conduction in axial direction is dominated by the heat exchange in  $\Omega$ . Moreover, the steel profiles are very long, so that we can view them to be endless. This justifies to neglect the heat conduction in axial direction and to regard a 2D heat equation in our reference domain  $\Omega$ . Related to this and to the real technical situation, we can assume that the intensity of any single spray nozzle is constant i.e. stationary with respect to the (outer) time.

We associate to each nozzle one part of the boundary  $\Gamma = \partial\Omega$  standing for its zone of influence. This leads to a partition of  $\Gamma$  into disjoint subdomains  $\Gamma_i$ ,  $i = 1(1)p$ . Denote by  $u_{ki}$  the cooling intensity of nozzle  $i$  in the group  $k$ ,  $k = 1(1)rM$ ,  $i = 1(1)p$ . Notice that this numbering covers some "phantom" nozzles in the air cooling areas. The numbers  $u_{ki}$  will be our *control variables*. In the case of *continuously* controllable nozzles we assume that the constraints  $0 \leq u_{ki} \leq 1$  are imposed for all  $k$  and  $i$ . The value 0 stands for an inactive nozzle, while 1 characterizes a nozzle spraying with maximal intensity. This implies  $u_{ki} \in \{0, 1\}$  as the set of admissible controls, if the nozzles can be only switched in (1) or off (0).

Adopting these notations, the mathematical model for the evolution of the temperature admits the following form, which is equivalent to that introduced in [7]: The temperature  $\vartheta$  in the profile is obtained from the nonlinear heat conduction problem

$$\begin{aligned} c(y)\rho(y) y_t &= \operatorname{div} (\lambda(y) \operatorname{grad} y) && \text{in } Q, \\ \lambda(y) \partial_n y &= \sum_{i,k} u_{ki} \chi(\Sigma_{ki}) \alpha(\cdot, y)(y_{fl} - y) && \text{in } \Sigma, \\ y(x, 0) &= y_0(x) && \text{in } \Omega, \end{aligned} \quad (2)$$

where  $Q = \Omega \times (0, T)$ ,  $\Sigma = \Gamma \times (0, T)$ ,  $\Sigma_{ki} = \Gamma_i \times (t_{k-1}, t_k)$ , and  $\chi(\Sigma_{ki})$  is the characteristic function of  $\Sigma_{ki}$ . In this setting,  $y_t$  and  $\partial_n y$  denote the derivatives  $\partial y / \partial t$  and  $\partial y / \partial n$  with respect to the time and the outer normal  $n$  at  $\Gamma$ , respectively. Moreover, the following quantities are used:

- $y = y(x, t)$  denotes the temperature at  $t \in [0, T]$  and  $x \in \Omega$ .  $T$  stands for the fixed terminal time.  $\Omega$  is a two-dimensional domain, and  $y_{fl}$  is the temperature of the cooling fluid.
- $u_{ki} \in \mathbb{R}$  are the control variables mentioned above. Outside the cooling segments the controls  $u_{ki}$  are taken zero to model heat isolation in the areas of air cooling. This is expressed by the characteristic function  $\chi(\Sigma_{ki})$  in the boundary condition of (2).
- The coefficients  $c$ ,  $\rho$ , and  $\lambda$  are functions of  $y$  denoting heat capacity, specific gravity, and heat conductivity, respectively. The function  $\alpha = \alpha(x, y)$  models the heat exchange coefficient. To find a good model for  $\alpha$  is a nontrivial task. In a simplified setting for cooling of cylindrical rods of steel, this issue was investigated by Zurdel and Brennecke [15]. Moreover, we refer to Rösch, [13].
- Our cooling process starts with the entrance temperature  $y_0 = y_0(x)$ .

The coefficients  $c$ ,  $\rho$ ,  $\lambda$  do not have appropriate properties of smoothness and monotonicity to show the unique solvability of the heat conduction problem. Moreover, the modelling of material changes during the subsequent heating and cooling of the steel is still partially open. The form (2) of the heat equation seems to give only an approximate picture of the temperature changes. Therefore, we do not discuss the question of existence and uniqueness of a solution to (2). Moreover, our computational method will mainly work with linearized versions. For these problems, the existence of a unique solution corresponding to a given vector of controls  $u = (u_{ki})$  is clear.

The restrictions on the control variables  $u_{ki}$  are alternatively given by

$$0 \leq u_{ki} \leq u_k \quad \text{or} \quad u_{ki} \in \{0, u_k\}, \quad (3)$$

$k = 1(1)rM$ ,  $i = 1(1)p$ , depending on whether we assume a continuous or discrete control strategy. Here,  $u_k = 0$  holds for  $k = (2j - 1)r(1)2jr$  with  $j = 1(1)M/2$  (air cooling) and  $u_k = 1$  otherwise (cooling segment).

The main aim of the cooling process is to reduce the temperature in the domain. Certainly, this can be expressed in various ways. In our model, the temperature should be minimized in a selection of points  $P_n \in \Omega$ ,  $n = 1(1)N$ , which characterize the hottest regions. In this way, the objective  $F$  is defined by the *linear* functional

$$F(y) = \sum_{n=1}^N a_n y(P_n, T) \quad (4)$$

with some positive weighting constants  $a_n$ .

In the model developed so far, most likely full intensity of all spray nozzles is optimal. However, this strategy is certainly wrong, since very large temperature differences would develop in  $\Omega$ . This would amount to a low quality of steel and possibly lead to large deformations of the profile. Therefore, we include a finite number of pointwise state constraints in the optimal control problem to bound the temperature differences in  $\Omega$ . Following [7], these constraints are given by

$$|y(R_\mu, t) - y(Q_\nu, t)| \leq \Theta_{\mu\nu}, \quad \mu = 1(1)N_R, \quad \nu = 1(1)N_Q. \quad (5)$$

In this setting,  $R_\mu$  and  $Q_\nu$  denote points from the closure of  $\Omega$ . For instance, the minimization points  $R_\mu := P_\mu$  can be chosen together with some comparison points  $Q_\nu$ . The situation of our test example is shown in Figure 2, where the points  $P_\nu$  and  $Q_\mu$  are numbered as follows:  $Q_1$  coincides with the origin. Following the boundary of the domain in mathematical positive sense, the next points are  $Q_2, \dots, Q_9, P_3, P_2, P_1$ . In this way,  $Q_9$  is located at the top, and  $P_1$  is the lowest among the  $P_i$ .

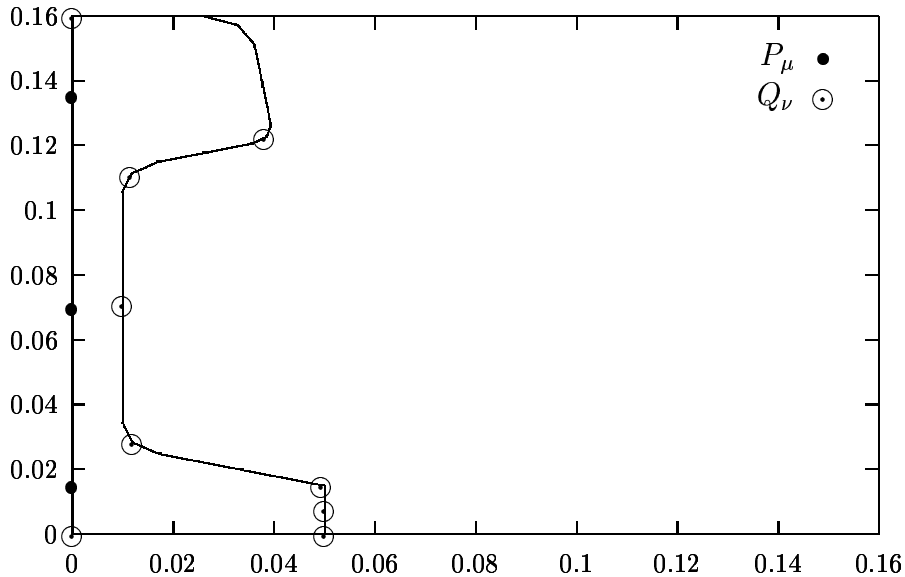


Figure 2: Points of Minimization and of Comparison

Now the definition of the control problem (P) is complete. For the continuous case, it reads as

$$(P) \quad \min F(y) = \sum_{n=1}^N a_n y(P_n, T)$$

subject to the state equation

$$\begin{aligned} c(y)\rho(y) y_t &= \operatorname{div} (\lambda(y) \operatorname{grad} y) && \text{in } Q, \\ \lambda(y) \partial_n y &= \sum_{i,k} u_{ki} \chi(\Sigma_{ki}) \alpha(\cdot, y)(y_{fl} - y) && \text{in } \Sigma, \\ y(x, 0) &= y_0(x) && \text{in } \Omega, \end{aligned}$$

and subject to the constraints on control and state

$$\begin{aligned} |y(R_\mu, t) - y(Q_\nu, t)| &\leq \Theta_{\mu\nu}, \quad \mu = 1(1)N_R, \quad \nu = 1(1)N_Q, \\ 0 &\leq u_{ki} \leq 1, \quad i = 1(1)p, \quad k = 1(1)K. \end{aligned}$$

A more detailed motivation can be found, for instance, in [7], [11]. We refer also to these papers for details of the numerical solution of the nonlinear parabolic initial-boundary value problem (2) by a finite-element-multigrid method. Let us briefly recall for convenience the main ideas characterizing the optimization technique of [7], [11].

The optimal control problem is difficult in several respects. The state equation is nonlinear, pointwise constraints on the state are given along with constraints on the controls, and the domain  $\Omega$  has a curved boundary. Besides the fact that the theory of optimal control problems for nonlinear distributed parameter systems with state-constraints is still far from being complete, the numerical solution is complicated. Readers interested in optimality conditions of first and second order for associated semilinear optimal control problems with state constraints are referred to our first paper in this volume.

Solving the heat equation by a sufficiently precise finite element multigrid method, a huge number of state variables appears in the discretized optimal control problem. However, compared with more academic problems discussed in literature, the technical circumstances of the cooling section show an essential advantage: The number of control variables is very low in comparison with the huge number of state variables. Therefore, we decided to use a direct method, where the controls appear as optimization variables, while the state equation is solved only for a certain number of basis controls. In [7], [11] an iterative method of feasible direction is developed. This algorithm proceeds as follows (below, the *control*  $u$  stands for the vector  $(u_{ki})$  of control variables):

1. Choose an admissible starting control vector  $u^0$  and compute the associated state  $y^0$ , put  $n = 0$ . Determine the active state constraints.
2. Linearize the state equation at  $y^n$  and  $u^n$ , solve it for each standard basis vector of controls. Then the state associated to an arbitrary admissible control can be obtained by superposition, see also the explanations in our first paper of this volume.

3. Express the state in the linearized optimal control problem as a linear image of the standard basis vectors using the results of step 2. Solve the associated linear optimization problem with respect to  $u$  by the Simplex method. Only active restrictions are considered in the optimization. The result is a new direction of descent  $\tilde{u}$ .
4. Put  $u^{n+1} = u^n + \gamma(\tilde{u} - u^n)$  and perform a line search with respect to  $\gamma$  while considering all state constraints. Define  $n = n + 1$  and go to 2.

This method of feasible direction is of gradient type. Computational tests have shown a quite robust behaviour. We stopped the iteration when the change of the controls was sufficiently small. The convergence rate is quite low. This is the characteristic behaviour of gradient methods. Moreover, the computing time to perform one step of the iteration was very high. Notice that linear partial differential equations are to be solved for each basis vector in step 2. Moreover, we have to solve some nonlinear equations arising from the line search.

Therefore, we propose a suboptimal strategy of instantaneous control type for approximately solving the problem (P). A comparison to the results of the iterative solution method shows a very fast and surprisingly exact behaviour. Furthermore, the method can be easily extended to the case of discrete 0-1 controls.

### 3 Suboptimal continuous and discrete methods

Let us first explain, how to accelerate the optimization procedure in the case of continuous controls. The main idea is of instantaneous control type and in some sense similar to the method, developed by Choi [1] and Hinze and Kunisch [5].

The first simplification is to *linearize the state equation* during certain intervals of time. Nevertheless, the resulting optimal control problem is still nonlinear. The point is the bilinear coupling of state and control in the boundary condition.

Therefore, we introduce the *heat flux*  $v := \lambda \partial_n y$  on the boundary as a new *auxiliary control vector*. After having determined the optimal heat flux, we derive an associated original control  $u$  by some heuristic formula. Notice that the heat flux has to be nonpositive during a cooling process.

**Remark:** This approach makes the optimization independent from the working hypothesis on the form of the boundary condition.

Introducing the heat flux as auxiliary control is combined with the idea to *shorten the time horizon* for minimizing the objective functional. This is the core of the instantaneous control technique. In the original formulation of the control problem, we have to achieve the minimal temperature at the final time  $T$ . Now we reduce the time horizon to certain small time intervals. The controls associated to the short interval under consideration are chosen to minimize the objective functional at the end of the time interval. In this way, we compute the (sub)optimal solution with respect to a short time horizon regardless of its

influence on future times. As a byproduct of linearization, we shall have to solve the state equation only on the associated short time intervals.

Next we shall explain the idea of instantaneous control in more detail. Select an index  $k \in \{1, \dots, K\}$  standing for a nozzle group. Suppose that the optimization process has already been performed for the nozzle groups  $1, \dots, k-1$ , that is up to the time  $t_{k-1}$ . Let  $y_{k-1} := y(x, t_{k-1})$  denote the temperature distribution obtained at time  $t_{k-1}$ . Freeze the coefficients of the heat equation at  $y_{k-1}$  on the whole time interval  $(t_{k-1}, t_k]$ ,

$$c = c(x) := c(y_{k-1}(x)), \quad \rho = \rho(x) := \rho(y_{k-1}(x)), \quad \lambda = \lambda(x) := \lambda(y_{k-1}(x)).$$

The associated time interval  $[t_{k-1}, t_k]$  is divided in  $L$  computational intervals  $I_{kl}$  of length  $\tau = (t_k - t_{k-1})/L$ ,  $I_{kl} = [t_{k-1} + (l-1)\tau, t_{k-1} + l\tau]$ ,  $l = 1(1)L$ . We require constant heat fluxes on  $I_{kl}$  and denote them by  $v_{kli}$ ,  $i = 1(1)p$ . The situation is shown in Figure 3.

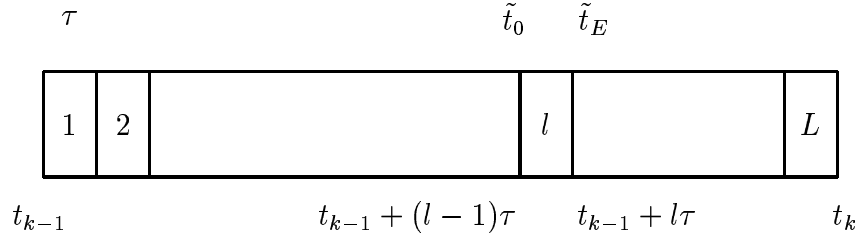


Figure 3: Partition of  $[t_{k-1}, t_k]$

Now we solve a *finite sequence of linear optimization problems*  $(P_{kl})$  associated to the small subintervals  $I_{kl}$ ,  $l = 1(1)L$ :

Having  $k-1$  fixed, regard now the partition of  $[t_{k-1}, t_k]$  for  $l = 1(1)L$ . Assume that the optimization has already delivered the solution up to the subinterval  $I_{k(l-1)}$  and regard the next subinterval  $I_{kl}$ . Denote by  $y_{k(l-1)}^I$  the initial temperature computed at the time  $\tilde{t}_0 := t_{k-1} + (l-1)\tau$  (we put  $y_{k0} := y_{k-1}$ ) and solve the following optimal control problem up to the time  $\tilde{t}_E := t_{k-1} + l\tau$ :

$(P_{kl})$      *Minimize*

$$F(y(\tilde{t}_E)) = \sum_{n=1}^N a_n y(P_n, \tilde{t}_E)$$

subject to the state equation

$$\begin{aligned} c(x)\rho(x) y_t &= \operatorname{div} (\lambda(x) \operatorname{grad} y) && \text{in } \Omega \\ \lambda(x) \partial_n y &= \sum_{i=1}^p v_i \chi(\Gamma_i) && \text{on } \Gamma \\ y(x, \tilde{t}_0) &= y_{k(l-1)}^I(x) && \text{in } \Omega, \end{aligned} \tag{6}$$



$t \in (\tilde{t}_0, \tilde{t}_E]$ , subject to the state constraints

$$|y(R_\mu, \tilde{t}_E) - y(Q_\nu, \tilde{t}_E)| \leq \Theta_{\mu\nu}, \quad (7)$$

$\mu = 1(1)N_R$ ,  $\nu = 1(1)N_Q$ , and to the restrictions on the control vector  $v = (v_i)$

$$q_{kli} \leq v_i \leq 0.$$

The choice of the bounds  $q_{kli}$  will be explained later. To unify the notation, let us consider air cooling areas as cooling segments as well. Here, the restriction  $u_{ki} = 0$  should imply  $q_{kli} = 0$ . We assume this. Then the only admissible control vector  $v = 0$  is optimal in air-cooling areas. This convention also holds for discrete strategies. We denote the obtained optimal solution by  $\bar{v}_i$ ,  $i = 1(1)p$ , and put  $v_{kli} := \bar{v}_i$ ,  $i = 1(1)p$ , to keep the index  $kl$  underlying the definition of  $(P_{kl})$ .

The solution of the optimal control problems  $(P_{kl})$  is the core of our suboptimal strategy. However, some further ideas are needed to make this strategy work effectively. The following points are still open: In the continuous case, we have to compute the original control vector  $u = (u_{ki})$  from the knowledge of the heat fluxes  $v_{kli}$ ,  $l = 1(1)L$ , which served as auxiliary variables. Further, the initial temperatures  $y_{k(l-1)}^I(x)$  must be computed in an appropriate way. In particular, we have to control the error caused by the effects of linearization. The bounds  $q_{kli}$  must be chosen.

**Remark:** The state constraints might be required at further instants of time. We check them only at the times  $\tilde{t}_E$ . Owing to this, small violations of the state constraints may occur inside the cooling areas.

*(i) Computation of auxiliary controls  $u_{kli}$ :*

Given the optimal heat fluxes  $v_{kli}$ , we define auxiliary controls  $u_{kli}$  as follows: Select some computational points  $x_i \in \Gamma_i$ . Take the mean value of

$$u_{kli}^- = v_{kli} / [\alpha(y(x_i, \tilde{t}_0))(y_{fl} - y(x_i, \tilde{t}_0))]$$

and

$$u_{kli}^+ = v_{kli} / [\alpha(y(x_i, \tilde{t}_E))(y_{fl} - y(x_i, \tilde{t}_E))],$$

that is

$$u_{kli} = \frac{u_{kli}^+ + u_{kli}^-}{2}. \quad (8)$$

*(ii) Computation of initial temperatures for  $I_{k(l+1)}$ :*

The initial temperature for the next optimization step can be determined on two ways: Solve the heat equation up to time  $\tilde{t}_E$  using the linear or nonlinear equation with boundary conditions of third kind inserting the computed controls  $u_{kli}$ . We preferred the nonlinear version. After having determined the auxiliary controls  $u_{kli}$ , we solve the *nonlinear* heat conduction problem

$$\begin{aligned} c(y)\rho(y) y_t &= \operatorname{div} (\lambda(y) \operatorname{grad} y) && \text{in } \Omega \\ \lambda(y) \partial_n y &= \sum_{i=1}^p u_{kli} \chi(\Gamma_i) \alpha(\cdot, y) (y_{fl} - y) && \text{on } \Gamma \\ y(x, \tilde{t}_0) &= y_{k(l-1)}^I(x) && \text{in } \Omega \end{aligned} \quad (9)$$

on  $[\tilde{t}_0, \tilde{t}_E]$ . Then we put  $y_{kl}^I(x) := y(x, \tilde{t}_E)$ . In other words, updating of temperatures is performed nonlinearly, while the optimization is done linearly.

(iii) Choice of the bounds  $q_{kli}$ :

The background to define  $q_{kli}$  is the relation

$$v_{kli} \approx u_{kli} \alpha(x, y(x, t))(y_{fl} - y(x, t)).$$

In view of this, inserting the upper bound 1 for  $u$  we define

$$q_{kli} = 1 \cdot \alpha(x_i, y_{k(l-1)}^I(x_i))(y_{fl} - y_{k(l-1)}^I(x_i)) \quad (10)$$

as the lower bound for  $v_{kli}$ .

(iv) Definition of original controls (continuous case):

The optimal control problems  $(P_{kl})$  are solved for  $k = 1(1)K$  (outer loop) and  $l = 1(1)L$  (inner loop). For each fixed index  $k$ , the problems  $(P_{kl})$  deliver the solutions  $u_{kli}$ ,  $l = 1(1)L$ ,  $i = 1(1)p$ , on the time intervals  $I_{kl}$ . Notice that, according to the given technical construction, only one control vector  $u_k = (u_{ki})$  has to be defined on  $[t_{k-1}, t_k]$ . This is done by the following heuristic formula, which turned out to be very useful:

$$u_{ki} = \frac{\sum_{l=1}^L l u_{kli}}{\sum_{l=1}^L l}. \quad (11)$$

This rule says that a change in the first small intervals of time can be compensated on the last intervals.

Now we explain the modifications of the continuous control strategy to the discrete counterpart. First of all, we have to increase the number of spray nozzles. This is to compensate for the loss of flexibility caused by restricting the controls to  $\{0, 1\}$ . We assume that each short time interval  $[t_{k-1} + (l-1)\tau, t_{k-1} + l\tau]$  corresponds to  $p$  spray nozzles located around the profile (= 1 nozzle group). In this way,  $L \cdot p$  spray nozzles are associated with the cooling segment passed during  $[t_{k-1}, t_k]$ , i.e., flexibility w. r. t. the value is substituted by flexibility in time. The corresponding spray intensities are  $u_{kli}$ ,  $l = 1(1)L$ ,  $i = 1(1)p$ . The heat fluxes  $v_{kli}$  (auxiliary variables) and the spray intensities  $u_{kli}$  are connected by the boundary condition (see (8)). As  $y$  varies in time and space, we cannot assume that  $u_{kli}$  and  $v_{kli}$  are constant on  $\Gamma_i \times (t_{k-1} + (l-1)\tau, t_{k-1} + l\tau)$  at the same time. However, if  $\tau$  is small we are justified to consider  $y$  to be almost constant. This also motivates the choice of the bounds  $q_{kli}$  (see (10)) as well as the synthesis rule (8), (11) in the continuous case. Moreover, in the discrete case the choice  $u \in \{0, 1\}$  corresponds directly to  $v \in \{q_{kli}, 0\}$  so that a synthesis rule is not needed.

By (i)–(iv), the whole interval  $[t_{k-1}, t_k]$  is processed. Now we proceed with the next interval  $[t_k, t_{k+1}]$ . In this way, we arrive after finitely many steps at

the final time  $T$ . Obviously, this procedure requires the numerical solution of many linear and nonlinear partial differential equations. On using the principle of superposition, we are able to considerably reduce the associated numerical effort. These details are explained in the next section.

## 4 Processing the subproblems

In each nozzle group, the number of controls is very low in comparison with the number of state variables arising from the finite element discretization. In our test example, we have  $p = 9$  control variables per nozzle group (there are 16 nozzles in each nozzle group, see Fig. 6, hence, by symmetry, the number of control variables is 9 in each group). In contrast to this, the number of state variables is some thousands. Therefore, in the optimization the state is eliminated by precomputing the response to each standard basis vector for the control, obtained from the linear equation: Regard, for  $k$  fixed, the interval  $[t_{k-1}, t_k]$ . For all  $i = 1(1)p$ , on  $[0, \tau]$  the response function  $y_{ki} = y_{ki}(x, t)$  is determined by

$$\begin{aligned} c(x)\rho(x) y_t &= \operatorname{div} (\lambda(x) \operatorname{grad} y) \\ \lambda(x) \partial_n y &= \chi(\Gamma_i) \\ y(x, 0) &= 0. \end{aligned}$$

These  $p$  systems have to be solved only once for the whole interval  $[t_{k-1}, t_k]$ . On the small subintervals  $I_{kl} = (t_{k-1} + (l-1)\tau, t_{k-1} + l\tau)$ , the temperature  $y$  is given by superposition,

$$y(x, t) = y^I(x, t) + \sum_{i=1}^p v_i y_{ki}(x, t - (l-1)\tau).$$

Here,  $y^I(x, t)$  is the fixed part, associated to the initial temperature and homogeneous boundary conditions. It is defined by

$$\begin{aligned} c(x)\rho(x) y_t &= \operatorname{div} (\lambda(x) \operatorname{grad} y) \\ \lambda(x) \partial_n y &= 0 \\ y(x, 0) &= y_{k(l-1)}^I(x). \end{aligned}$$

The second part represents the contribution associated to the controls  $v_i$ . During the optimization process, only the fixed part has to be updated from one subinterval to the next one. Then the optimization problem on  $I_{kl}$  reads for the case of *continuously* controllable nozzles

( $\mathbf{P}_{kl}$ )      *Minimize*

$$\sum_{n=1}^N \sum_{i=1}^p c_{in} v_i$$

subject to

$$\begin{aligned} \sum_{i=1}^p v_i a_{i\mu\nu} &\leq \Theta_{\mu\nu} - b_{\mu\nu} \\ - \sum_{i=1}^p v_i a_{i\mu\nu} &\leq \Theta_{\mu\nu} + b_{\mu\nu} \\ q_i &\leq v_i \leq 0, \end{aligned}$$

$i = 1(1)p$ , where

$$\begin{aligned} c_{in} &= c_{kin} = y_{ki}(P_n, \tau) \\ a_{i\mu\nu} &= a_{ki\mu\nu} = y_{ki}(R_\mu, \tau) - y_{ki}(Q_\nu, \tau) \\ b_{\mu\nu} &= b_{kl\mu\nu} = y^I(R_\mu, \tilde{t}_E) - y^I(Q_\mu, \tilde{t}_E). \end{aligned}$$

The bounds  $q_i = q_{kli}$  are defined according to (10). This linear programming problem is solved by the Simplex method. Its optimal solution  $\bar{v} = (\bar{v}_i)$  is denoted by  $\bar{v}_{kli}$ ,  $i = 1(1)p$ , to preserve the index  $kl$ . Notice that the numbers  $c_{in}$ ,  $a_{i\mu\nu}$  have to be computed only once on  $[t_{k-1}, t_k]$ , while the  $b_{\mu\nu}$  and  $q_i$  depend on  $l$ , hence they must be updated on all subintervals.

For discrete strategies, we arrive at linear *integer* programming problems of the same structure like above, which have to be solved by appropriate methods.

$$\begin{aligned} \min \quad & \sum_{n=1}^N \sum_{i=1}^p c_{in} v_i, \\ \text{subject to} \quad & \\ & \sum_{i=1}^p v_i a_{i\mu\nu} \leq \Theta_{\mu\nu} - b_{\mu\nu} \\ & - \sum_{i=1}^p v_i a_{i\mu\nu} \leq \Theta_{\mu\nu} + b_{\mu\nu} \\ & v_i \in \{q_i, 0\}, \quad i = 1, \dots, p. \end{aligned}$$

Strictly speaking, this is not a binary problem, since  $q_m \neq 1$  in general. If particular discrete optimization methods are based on a binary structure, the problem must be transformed appropriately. Since  $q_m$  is updated after each time step  $\tau$ , this means changing the matrix of constraints and the coefficients of the objective in each step. If the discrete method needs a special preprocessing of these data, this has to be repeated for each subproblem.

During the computations we observed effects of ill-posedness for small values of  $\tau$  close to the time step for solving the PDEs. For instance, even in the continuous case, we observed that some controls were switching from 0.4 to 1.0 and reverse by changing the discretization of time. To overcome this problem, instead of using the original linear objective functional given above, we minimized in all cases the *linearly regularized objective*

$$\text{Min} \quad \sum_{n=1}^N \sum_{i=1}^p c_{in} v_i + \varepsilon \sum_{i=1}^p v_i$$

subject to the constraints given above. This trick stabilized the computed optimal controls.

## 5 Numerical results

### 5.1 The test example

One of our standard test examples is the cooling of rail profiles. Following [7], [11], we consider the domain shown in Figure 5 with a moderate discretization. The concrete formulas for the coefficients  $c$ ,  $\rho$ ,  $\lambda$ ,  $\alpha$  are adopted from these papers. All other data were transmitted by the Mannesmann–Demag–Sack GmbH.

We restrict ourselves to the situation of [7]. That is, we consider 3 minimization points  $P_n$  on the axis of symmetry and take them as comparison points too, that is  $R_\mu := P_\mu$ . 9 points of comparison are chosen on the boundary. Their location is shown in Figure 2. The temperature at these points is compared with the temperature at the minimization points according to the table below.

Point	compared with
$P_1$	$Q_1, Q_2, Q_3, Q_4$
$P_2$	$Q_4, Q_5, Q_6,$
$P_3$	$Q_6, Q_7, Q_8, Q_9$

Table 1: Comparison points

In the test example, we regard a cooling line composed of one cooling segment followed by one air cooling area both with length equivalent to 15 seconds. Hence our cross section  $\Omega$  passes the whole plant in 30 seconds. The cooling segment contains two blocks. In the continuous case, each block is identified with one nozzle group, whereas in the discrete case we have essentially more nozzle groups and each block corresponds to the time interval for freezing the coefficients  $c$ ,  $\rho$  and  $\lambda$ . Each nozzle group consists of 16 spray nozzles, hence by symmetry we have 9 control variables, see Fig. 6. Following the notation of Section 2 we have  $m = 2$ ,  $r = 2$ ,  $p = 9$ . The geometry is shown in Figure 4. According to the general setting, for  $t_1$  we get the value 7.5 seconds.

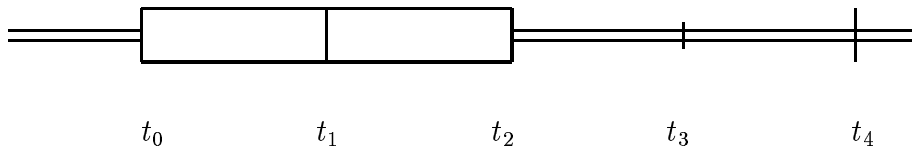


Figure 4: Test geometry

The partition of the boundary  $\Gamma$  into parts  $\Gamma_i$  is roughly indicated in Figure 6. For the exact geometry of the rail profile we refer to Figure 2.

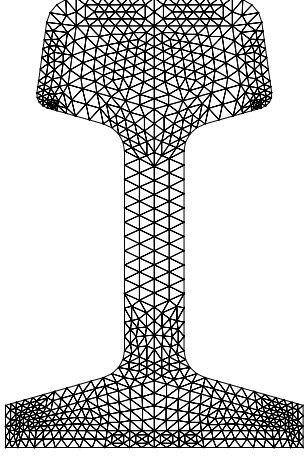


Figure 5: The rail profile

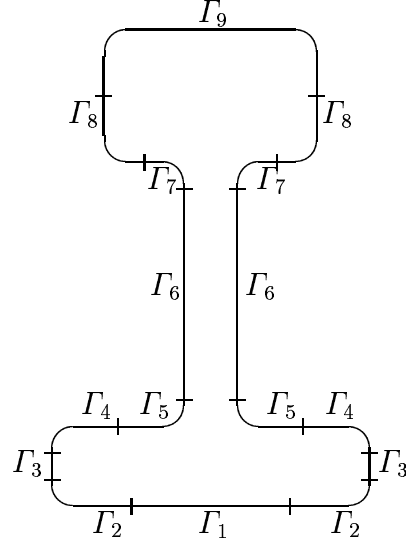


Figure 6: Partition of  $\Gamma$

The parabolic state equation was solved by a Crank-Nicholson scheme in time and a 3-step FEM multigrid algorithm for the elliptic subproblems. The initial value is chosen as in [7] assuming constant temperatures in 3 areas.

For presenting test results, we proceed as follows: In a first part we compare the suboptimal strategy with the method of feasible directions in the case of continuous controls. In a second part we compare between continuous and discrete cooling strategies, in particular we discuss the lack of efficiency using discrete 0-1 nozzles. Moreover, we present results for improving efficiency of discrete strategies by applying nozzles of *lower* size, i.e. of *lower* maximal cooling intensity.

## 5.2 Feasible directions versus suboptimal strategy

According to subsection 5.1, we consider the following test problem **(E)**:

$$\min F(y) = \sum_{n=1}^3 a_n y(P_n, T) \quad (12)$$

subject to

$$\begin{aligned} c(y)\rho(y) y_t &= \operatorname{div} (\lambda(y) \operatorname{grad} y) \\ \lambda(y) \partial_n y &= \sum_{i,k} u_{ki} \chi(\cdot, \Gamma_i) \alpha(y)(y_{fl} - y) \\ y(x, 0) &= y_0(x), \end{aligned} \quad (13)$$

to the control constraints

$$0 \leq u_{ki} \leq 1, \quad (14)$$

$k = 1, 2$ ,  $i = 1(1)9$ , (cooling segment),  $u_{ki} = 0$ ,  $k = 3, 4$ ,  $i = 1(1)9$  (air cooling area), and subject to the state constraints

$$|y(P_\mu, t) - y(Q_\nu, t)| \leq \Theta_{\mu\nu}, \quad \mu = 1(1)3, \quad \nu = 1(1)9, \quad (15)$$

where  $T = 30$  sec, and we have  $18 = 2 \cdot 9$  controls acting for 7.5 seconds on different time intervals and on different boundary parts. We have chosen the values  $\Theta_{\mu\nu} = |P_\mu - Q_\nu| \cdot 8000$  K/m, if the point  $P_\mu$  is compared with the point  $Q_\nu$  according to Table 1, and  $\Theta_{\mu\nu} = \infty$  otherwise. In the computations we omit the constraints, where  $\Theta_{\mu\nu} = \infty$ . Furthermore, we take the weights  $a_1 = a_3 = 3$  and  $a_2 = 1$ .

In the test runs of this subsection we worked with a time step of 0.75 seconds to solve the PDE. Therefore, we splitted each interval  $[t_{k-1}, t_k]$  into 10 parts having just this length  $\tau = 0.75$  sec. Obviously, this is the smallest length we can use for computational intervals in our case. In this way, we got the discretization of time  $0 = t_0 < t_0 + \tau < \dots < t_0 + 10\tau = t_1 < \dots < t_1 + 10\tau = t_2 < \dots < T$ , where  $T = 30$  sec and  $\tau = 0.75$  sec.

The fast suboptimal strategy determines the solution in a very short time. Moreover, it is a direct method. In particular, no admissible initial control  $u_0$  is needed. We list the computational results for the values  $L = 1, 5, 10$  in Table 2. The CPU time was about 2 minutes on a workstation HP Apollo 9000. Table 2 contains the computed controls and the corresponding values of the cost functional together with the temperature in the minimization points. Our suboptimal method was applied for different numbers of computational intervals. Our values show the surprising effect that more (but smaller) computational intervals increase the precision of our method while decreasing the computational time. The reason for the gain of speed is that computing the response functions is cheaper on shorter intervals.

The results are compared with those obtained by the method of feasible directions in [7]. To that aim this slow iterative method was started at controls computed by our suboptimal method for the largest number of computational intervals. Nevertheless, to get the marginal improved "optimal" values in the last column of the table, the iterative method required 177 iteration steps. Hence we needed 2.5 days to get this slightly better result. **One** iteration by the method of [7] needs a between five and ten times longer computational time than our whole method. Altogether, accuracy and running time of the fast method of instantaneous control are very convincing.

$r_c$	1	5	10	Method of [7]
$U_{11}$	0.351402	0.354894	0.357386	0.361015
$U_{12}$	1.000000	0.798217	1.000000	1.000000
$U_{13}$	0.118034	0.588312	0.462750	0.510719
$U_{14}$	1.000000	1.000000	1.000000	1.000000
$U_{15}$	1.000000	1.000000	1.000000	1.000000
$U_{16}$	0.336405	0.368480	0.376729	0.383220
$U_{17}$	0.562985	0.606946	0.612365	0.644712
$U_{18}$	0.572915	0.661840	0.686257	0.720357
$U_{19}$	0.434374	0.458182	0.454216	0.488881
$U_{21}$	0.398711	0.407742	0.413433	0.422056
$U_{22}$	1.000000	0.896221	0.927565	0.935165
$U_{23}$	0.114328	0.079897	0.036162	0.077026
$U_{24}$	1.000000	0.957728	0.977744	0.982834
$U_{25}$	1.000000	1.000000	1.000000	1.000000
$U_{26}$	0.378044	0.387829	0.386588	0.384954
$U_{27}$	0.581319	0.569530	0.565634	0.578580
$U_{28}$	0.516497	0.456389	0.449471	0.469555
$U_{29}$	0.437347	0.429484	0.428212	0.436120
$y(T, P_1)$	781.909	781.855	781.055	780.630
$y(T, P_2)$	755.870	752.048	751.399	750.944
$y(T, P_3)$	854.393	853.167	853.106	851.579
$F(y)$	5664.776	5657.115	5653.881	5647.572
CPU	208 sec	106 sec	100 sec	1200 sec / It.

Table 2: Performance of the suboptimal strategy

However, there appear small problems with violating the state constraints. Therefore, after the first iterations the method of [7] still delivered a solution with considerably larger value than that of our fast approximate solution. The level of violation is low (0.3 K at most). In our opinion, this is sufficiently small to accept the computed control. Nevertheless, one should carefully observe this problem in more complicated situations. For more details we refer to [14].

### 5.3 Continuous versus discrete suboptimal strategies

In the continuous case,  $[t_{k-1}, t_k]$  contains one nozzle group, where the nozzles can admit all intensities in  $[0, 1]$ . The interval  $[t_{k-1}, t_k]$  was splitted into  $L$  subintervals of length  $\tau$ , which served as auxiliary subintervals. Now we compare the results with the following discrete situation: To each subinterval we associate one nozzle group, i.e. we have  $L = 10$  times more nozzles in  $[t_{k-1}, t_k]$ . In other words, 18 *continuously* controllable nozzles are replaced by 180 nozzles. However, these nozzles can only admit the intensities 0 (off) and 1 (on), and they influence the profile for a shorter time, i.e. only for  $\tau = (t_k - t_{k-1})/10$ .

The integer programming subproblems were solved by complete enumeration. The size of the subproblems is so small that this method was faster than standard branch and bound algorithms. We obtained computational times close to the ones for the continuous case. This shows that the solution of the integer problem needs approximately the same time as the simplex method, essentially faster than the



time needed by the method of feasible directions. Optimal values and computing times are compared in Table 3. We observed that data generation, in particular computation of response functions, is stronger sensitive with respect to the length of time step than the solution of the state equation. We had to find a reasonable compromise between accuracy and computing time. In Table 3, different choices of time steps are compared for solving the instantaneous control problem:

In all cases I-III (dis=discrete, con=continuous), the optimization subproblems are solved on time horizons of length  $\tau$ . However, we do not update all coefficients of the problem after each time step  $\tau$ . The coefficients  $c_{in}$  of the objective and the matrix  $A = (a_{i\mu\nu})$  of the constraints are updated only after larger intervals of time (in our test example after  $10\tau$ ), while the right hand sides  $\Theta_{\mu\nu} \pm b_{\mu\nu}$  of the constraints are updated after each time step  $\tau$ . In case I,  $\tau$  is used as the step length to solve the parabolic equation for updating the state and the  $b_{\mu\nu}$  as well as for the generation of the optimization data  $c_{in}$ ,  $a_{i\mu\nu}$  via response functions. In case II we used a smaller time step  $\tau_{II} = \tau/5$  for all computations. Case III proceeds as case I with respect to the update of the state, but the coefficients of the matrix and the objective are computed with higher precision by the time step  $\tau/5$ .

	I dis	II dis	III dis	I con	II con	III con	Method of [7]
$F(y)$	5841.1	5848.8	5853.2	5641.8	5643.3	5653.7	5647.6
CPU	122. sec	431 sec	177 sec	124 sec	433 sec	180 sec	59 h (177 It.)

Table 3: Optimal values and computing times

Table 4 contains the associated optimal controls. In the continuous cases I-III con, the values  $u_{ki}$ ,  $k = 1, 2$ ,  $i = 1(1)9$ , express the intensity of nozzle  $i$  in group  $k$ . In the discrete cases, the reader would expect  $K \cdot p \cdot L = 2 \cdot 9 \cdot 10$  values  $u_{kli} \in \{0, 1\}$ . To avoid the associated large table and to make the results comparable with the continuous case, the columns I dis - III dis contain the mean values, defined by formula (11),

$$u_{ki} = \frac{\sum_{l=1}^{10} l u_{kli}}{\sum_{l=1}^{10} l}, \quad i = 1(1)9.$$

$r_c$	I dis	II dis	III dis	I con	II con	III con
$U_{11}$	0.14545	0.18182	0.18182	0.35739	0.35719	0.34315
$U_{12}$	0.74545	0.78182	0.78182	1.00000	1.00000	1.00000
$U_{13}$	0.45454	0.32727	0.32727	0.46275	0.41935	0.39777
$U_{14}$	1.00000	1.00000	1.00000	1.00000	1.00000	1.00000
$U_{15}$	1.00000	1.00000	1.00000	1.00000	1.00000	1.00000
$U_{16}$	0.00000	0.00000	0.00000	0.37673	0.36948	0.35291
$U_{17}$	0.47273	0.34545	0.40000	0.61237	0.60966	0.58313
$U_{18}$	0.61818	0.43636	0.43636	0.68626	0.67156	0.66524
$U_{19}$	0.27273	0.20000	0.20000	0.45422	0.45254	0.43632
$U_{21}$	0.18182	0.23636	0.25455	0.41343	0.41091	0.39926
$U_{22}$	0.98182	0.80000	0.80000	0.92756	0.91320	0.91700
$U_{23}$	0.01818	0.01818	0.01818	0.03616	0.03209	0.02941
$U_{24}$	1.00000	0.81818	0.81812	0.97774	0.96000	0.96622
$U_{25}$	1.00000	1.00000	1.00000	1.00000	1.00000	1.00000
$U_{26}$	0.00000	0.00000	0.00000	0.38659	0.38420	0.36980
$U_{27}$	0.54545	0.45455	0.54545	0.56569	0.56630	0.55394
$U_{28}$	0.38182	0.30909	0.41818	0.44947	0.44810	0.44394
$U_{29}$	0.29091	0.27273	0.27273	0.42821	0.42644	0.42035

Table 4: Optimal controls (all variants)

It is quite natural that integer controls are not so flexible as the continuous ones. Even by using ten times more nozzles as in the continuous case, there is an essential lack of efficiency causing a temperature difference of almost 30 K in every "hot spot"  $P_n$  selected for the objective. Due to the state constraints, some of the nozzles ( $u_{16}$ ,  $u_{26}$ ) must kept switched off during the whole process, which is the main reason for the gap. Nevertheless, using the same number of nozzles of **lower** size can improve the efficiency of discrete cooling. A careful comparison of the optimal controls in Table 4 shows the main reason for the lack of efficiency in the discrete case: In particular, nozzle 6 is never active in all variants, while in the continuous case a moderate and almost **uniform** cooling takes place. This can be observed from the solution of the subproblems, because it holds  $0.365 \leq u_{16} \leq 0.375$ , and  $0.38 \leq u_{26} \leq 0.39$  for all  $l = 1(1)10$ . Obviously, the constraints for nozzle 6 are too strong for cooling with intensity 1, even if the time of cooling is very short. Consequently, no cooling is the only admissible control. This seems to be a typical difficulty for discrete strategies. However, the comparison with the continuous problem shows the possibility of an almost uniform cooling, if the maximal intensity of the nozzle is reduced to  $i_6 = 0.35$ . In Table 5 we present two different cases (data generation and update by refined stepsize  $\tau/3$ ): The first column contains the results, where the maximal cooling intensity of nozzle 6 was reduced to 0.35, while the others still had the size 1.0 as before. The values in the second column correspond to the following maximal cooling intensities  $i_1, \dots, i_9$  for the nozzle 1(1)9:  $i_1 = 0.5$ ,  $i_2 = 0.8$ ,  $i_3 = 0.4$ ,  $i_4 = 1$ ,  $i_5 = 1$ ,  $i_6 = 0.35$ ,  $i_7 = i_8 = i_9 = 0.5$ . This version is called the refined strategy. Notice that these intensities are fixed in advance by our experience from the continuous case. The last two columns are added for a comparison with the standard choice of maximal intensity 1.0 for all nozzles.

	$i_6 = 0.35$	refined	con	dis
$U_{11}$	0.18182	0.30175	0.35733	0.18182
$U_{12}$	0.78182	0.80000	1.00000	0.78182
$U_{13}$	0.32727	0.40000	0.42245	0.32727
$U_{14}$	1.00000	1.00000	1.00000	1.00000
$U_{15}$	1.00000	1.00000	1.00000	1.00000
$U_{16}$	0.35000	0.35000	0.36983	0.00000
$U_{17}$	0.40000	0.50000	0.60945	0.34544
$U_{18}$	0.43636	0.50000	0.67217	0.43636
$U_{19}$	0.18182	0.43778	0.45205	0.18182
$U_{21}$	0.21818	0.36526	0.41118	0.21818
$U_{22}$	0.80000	0.80000	0.91482	0.80000
$U_{23}$	0.01818	0.10964	0.03246	0.01818
$U_{24}$	1.00000	1.00000	0.96173	0.81818
$U_{25}$	1.00000	1.00000	1.00000	1.00000
$U_{26}$	0.35000	0.35000	0.38444	0.00000
$U_{27}$	0.36364	0.50000	0.56625	0.45454
$U_{28}$	0.49091	0.50000	0.44818	0.49091
$U_{29}$	0.27273	0.35566	0.42653	0.27273
$F(y)$	5746.41	5689.95	5642.87	5847.74

Table 5: Optimal controls for the refined strategy

The refined strategy essentially improves the standard discrete method, although the efficiency of the continuous strategy cannot be reached completely. Moreover, we observed the following: Nozzles with reduced intensities prevent the controls from chattering - the number of switches between consecutive nozzles is reduced. Some of the nozzles were active all the time. For some more details, including resulting different temperature distributions of the profile, we refer to [3].

**Conclusions:** The instantaneous control technique is successful for continuous and discrete control strategies. In our example, it is able to deal with discrete cooling strategies in almost the same time as for the continuous method. The application of fixed maximum intensity 1.0 turned out to be insufficient: Even essentially more nozzles cannot deliver the same final temperature as the continuous strategy. Using nozzles of lower size can overcome this problem. The solution of the continuous problem is helpful to design the size of nozzles.

## References

1. H. Choi. Suboptimal control of turbulent flow using control theory. In *Proceed. Sympos. Math. Modelling of Turbulent Flows*, Tokio, 1995.
2. H. W. Engl, T. Langthaler, and P. Mansellio. An inverse problem for a nonlinear heat equation connected with continuous casting of steel. In K.-H. Hoffmann and W. Krabs, editors, *Optimal control of partial differential equations*, pages 67–90, Basel, 1987. Birkhäuser.
3. K. Eppler and F. Tröltzsch. Discrete and continuous optimal control strategies in the selective cooling of steel. Preprint 01–3, DFG-Forschungsschwerpunkt "Real-time optimization of large systems", 2001.
4. W. Grever. A nonlinear parabolic initial boundary value problem modelling the continuous casting of steel. *ZAMM*, 78:109–119, 1998.

5. M. Hinze and K. Kunisch. On suboptimal strategies for the Navier-Stokes equations with continuous casting of steel. In *Contrôle et Équations aux Dérivées Partielles*, pages 181–198. ESAIM: proceedings, vol. 4, 1998.
6. D. Hömberg and J. Sokolowski. Optimal control of laser hardening. Preprint 315, Weierstraß Institute of Applied Analysis and Stochastics Berlin, 1997.
7. R. Krengel, R. Standke, F. Tröltzsch, and H. Wehage. Mathematisches Modell einer optimal gesteuerten Abkühlung von Profilstählen in Kühlstrecken. Preprint 98–6, TU Chemnitz, Fakultät für Mathematik, 1996.
8. E. Laitinen and P. Neittaanmäki. On numerical solution of the continuous casting process. *J. of Engineering Mathematics*, 22:335–354, 1988.
9. G. Landl and H. W. Engl. Optimal strategies for the cooling of steel strips in hot strip mills. *Inverse Problems in Engineering*, 2:102–118, 1995.
10. F. Leibfritz and E. W. Sachs. Numerical solution of parabolic state constraint control problems using SQP- and interior-point-methods. In W.W. Hager, editor, *Large scale optimization*, pages 245–258, Dordrecht, 1994. Kluwer Academic Publishers B.V.
11. R. Lezius and F. Tröltzsch. Theoretical and numerical aspects of controlled cooling of steel profiles. In H. Neunzert, editor, *Progress in Industrial Mathematics at ECMI 94*, pages 380–388. Wiley-Teubner, 1996.
12. P. Neittaanmäki. On the control of the secondary cooling in the continuous casting of steel. In K.-H. Hoffmann and W. Krabs, editors, *Optimal control of partial differential equations*, pages 161–178, Basel, 1987. Birkhäuser.
13. A. Rösch. Identification of nonlinear heat transfer laws by optimal control. *Num. Funct. Analysis and Optimization*, 15(3&4):417–434, 1994.
14. F. Tröltzsch and A. Unger. Fast solution of optimal control problems in the selective cooling of steel. *ZAMM*, 81:447–456, 2001.
15. K. Zurdel and N. Brennecke. *Untersuchungen zum Wärmeübergang bei der Wasserkühlung von Feinstahl und Walzdraht*. PhD thesis, Technische Hochschule Magdeburg, 1974.